Supplement of The Cryosphere, 19, 6187–6205, 2025 https://doi.org/10.5194/tc-19-6187-2025-supplement © Author(s) 2025. CC BY 4.0 License.





Supplement of

Sensitivity of Totten Glacier dynamics to sliding parameterizations and ice shelf basal melt rates

Yiliang Ma et al.

Correspondence to: Liyun Zhao (zhaoliyun@bnu.edu.cn) and John C. Moore (john.moore.bnu@gmail.com)

The copyright of individual parts of the supplement might differ from the article licence.

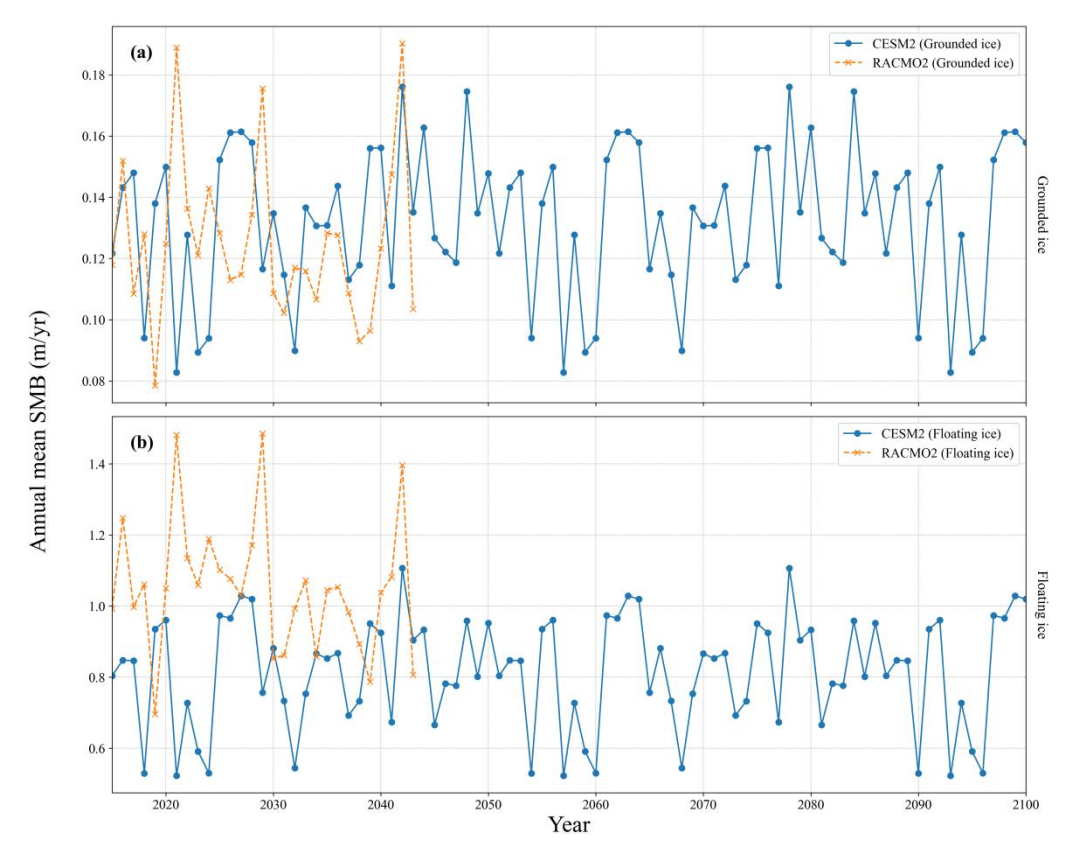


Fig. S1. The SMB time series (blue curve) used for the period 2015-2100 in our experiments, consisting of repeated 1995-2030 CESM2 output, which is compared with the 1995-2023 SMB from RACMO2.4p1 data (orange dashed curve; Van Dalum et al., 2024).

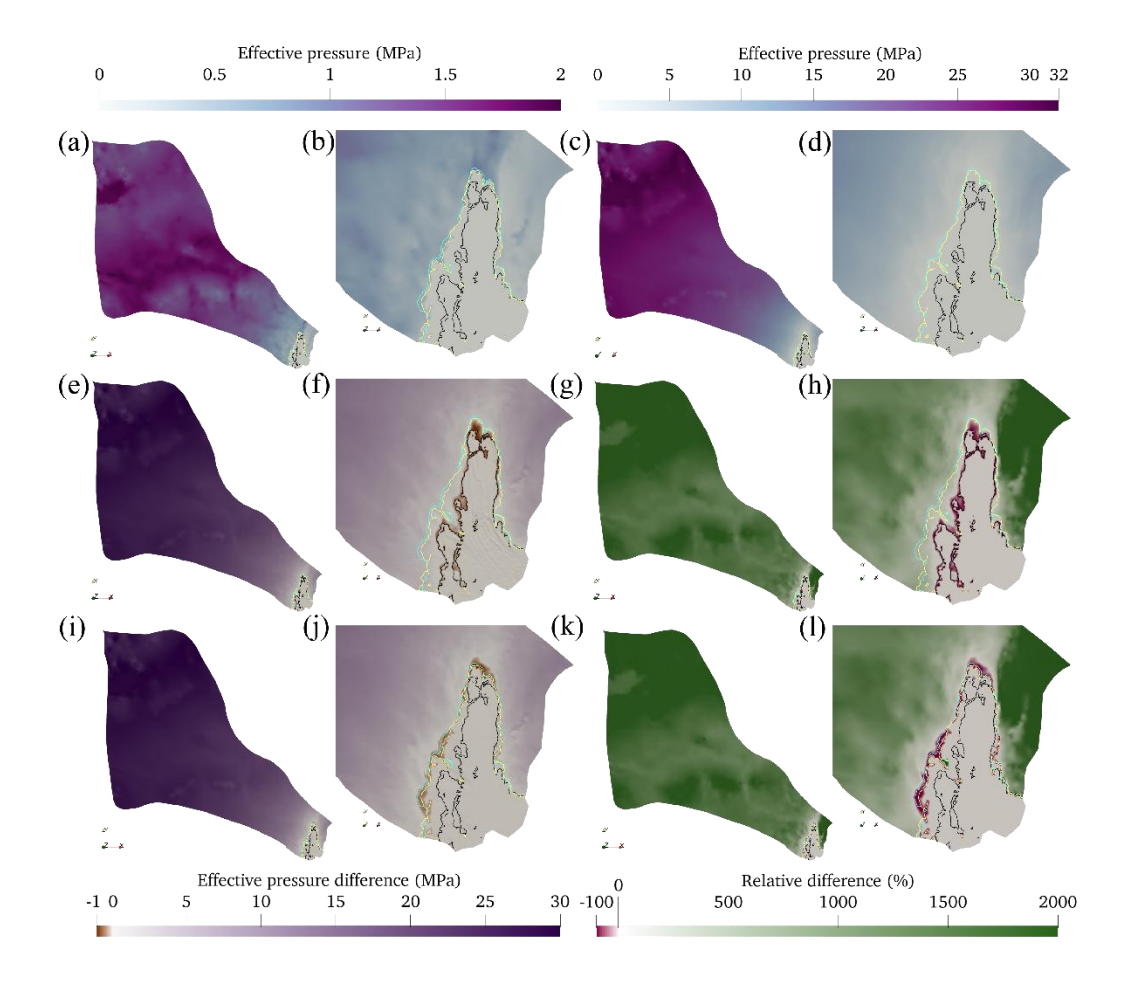


Fig. S2. Effective pressure set to 5% of overburden (a, b) and effective pressure assuming perfect hydrostatic connection and subglacial elevations (c, d) in the year 2050 from the experiment C_{m80} . Difference (e, f, i, j) and relative difference (g, h, k, l) between 5% of overburden and perfect connection at the beginning (e-h) and the end (i-l) of the 35 years simulation. The yellow and cyan curves represent the grounding line positions under 5% of overburden and perfect connection respectively after 35 years simulation. Note the different colorbar scales for (a, b) and (c, d).

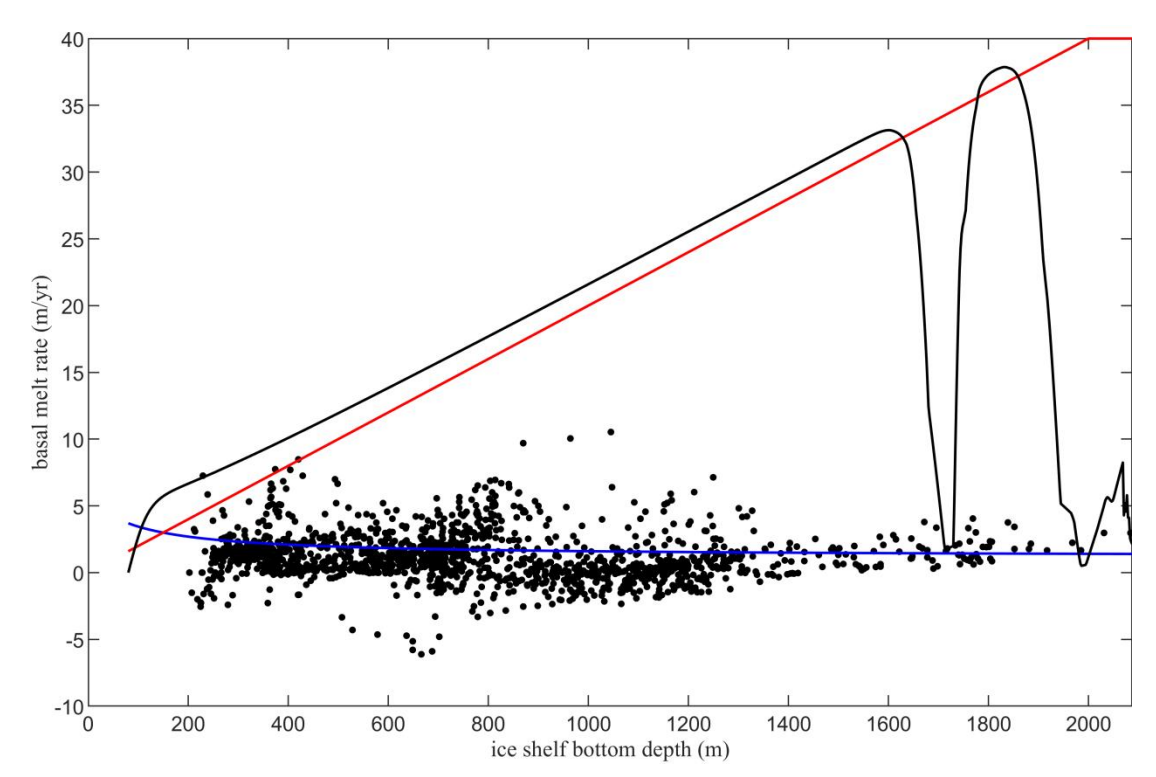


Fig. S3. Basal melt parameterization. Positive value of basal melt rate are melting and negative freezing rates. Whole Antarctic Ocean Model (WAOM v1.0; Richter et al., 2022) simulated basal melt rate (points) - which are far lower than spatially averaged satellite observational rates - see Section 3.3. The blue curve shows Eq. (17) tuned to WAOM modelled sub-shelf basal melt rates (d0 = 100 m). The red curve is parameterized to account for the observed high melt rates in the deep water (Eq. (18) with a M_{max} = 40 m yr⁻¹). The sub-shelf melt is set to zero for ice shelf bottom depth less than 80 m (Eq. (20)). The black curve is the total sub-shelf basal melt (Eq. (21)) with water column thickness along the flowline FL1.

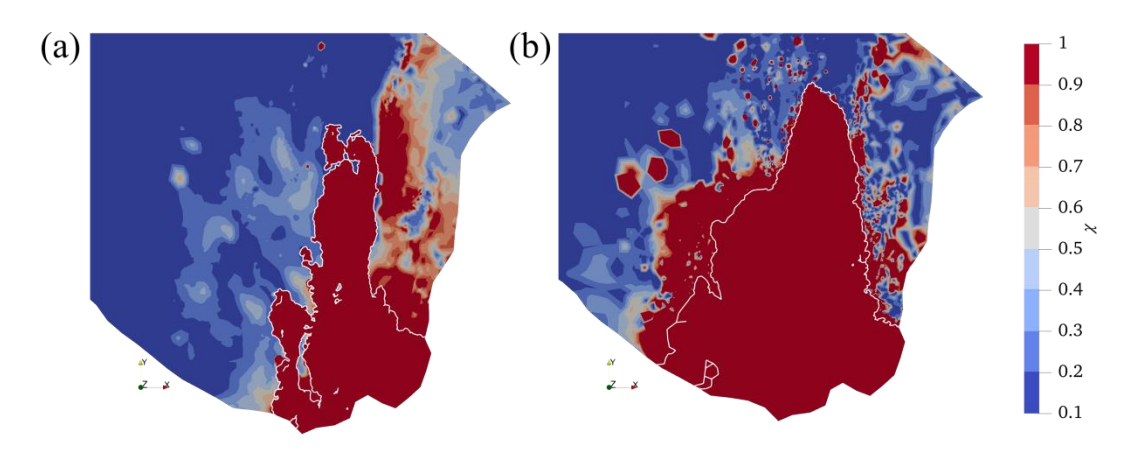


Fig. S4. The χ value near the grounding line in the year 2015 (a) and 2100 (b) confined to [0.1, 1.0] in the experiment C_{m80}. The white curve is the grounding line. Ignore the value on the ice shelf, which is not applied.

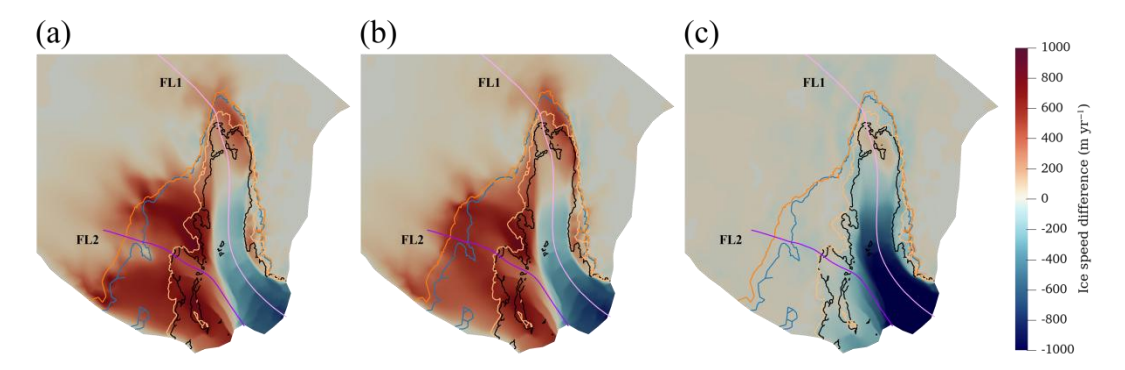


Fig. S5. The surface ice speed change from the year 2015 to 2100 (2100 minus 2015) in the experiments C_{m80} (a), LW_{m80} (b) and NW_{m80} (c). The solid black line represents the initial grounding line position in the year 2015. The orange, blue and pink curves represent grounding line positions in the year 2100 from experiments C_{m80} , LW_{m80} and NW_{m80} in the sliding parameterization group (Table 3).

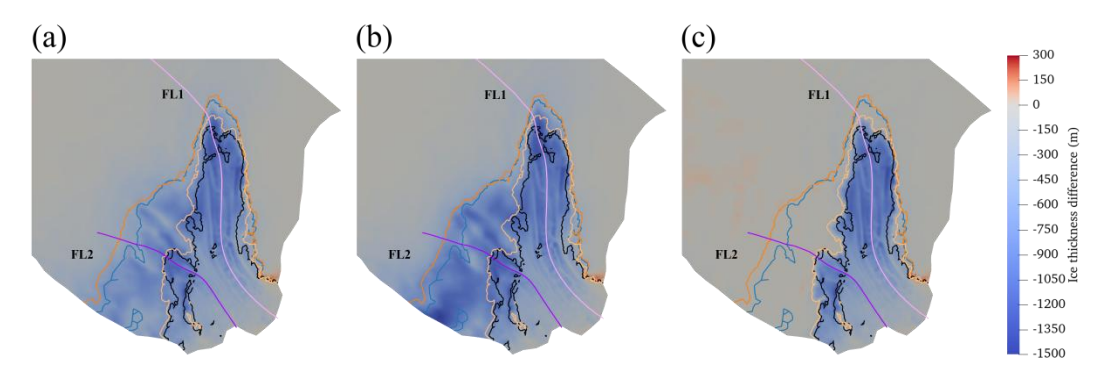


Fig. S6. The same as in Fig. S5 but for ice thickness change.

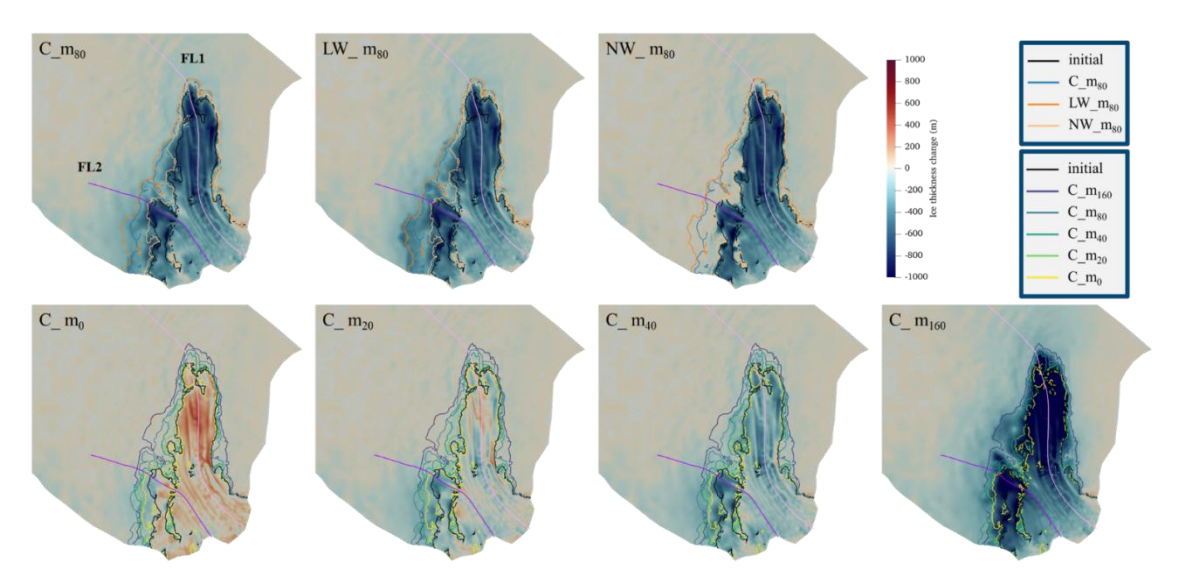


Fig. S7. Ice thickness change from 2015 to 2050 (2050 minus 2015) in different experiments as labeled. The black curve represents the initial grounding line position in the year 2015, and the coloured curve (see legend) represents the grounding line position in the year 2050 in different experiments.

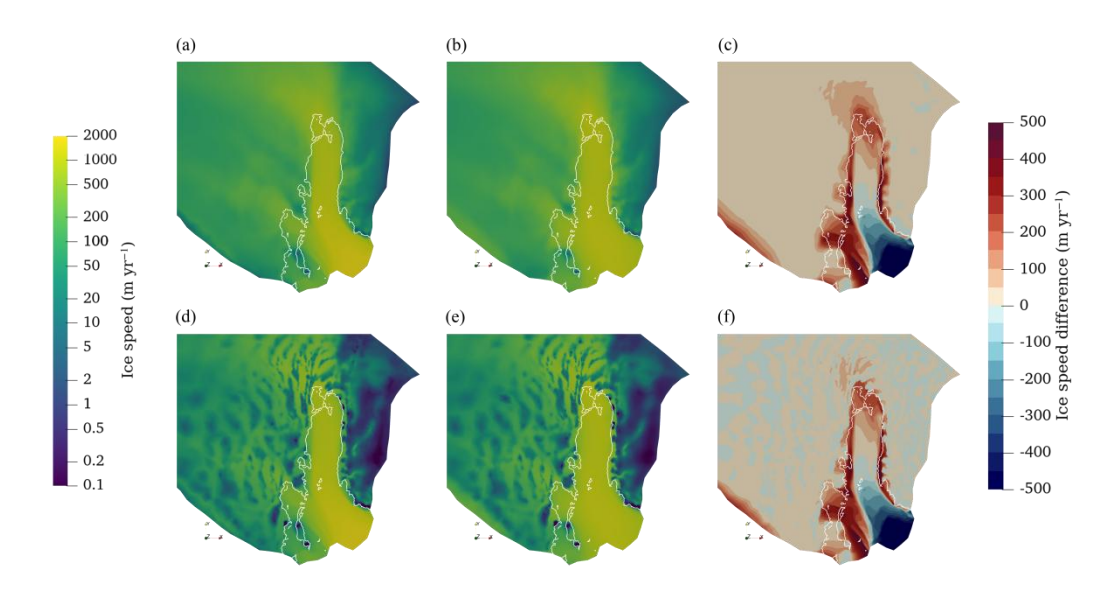


Fig. S8. The simulated surface (the first row) and basal (the second row) ice speed in steady state simulation using full-Stokes model (a, d) and Blatter-Pattyn model (b, e) restarting from the steady state result of full-Stokes model, and their difference (c, f) which is Blatter-Pattyn minus full-Stokes.

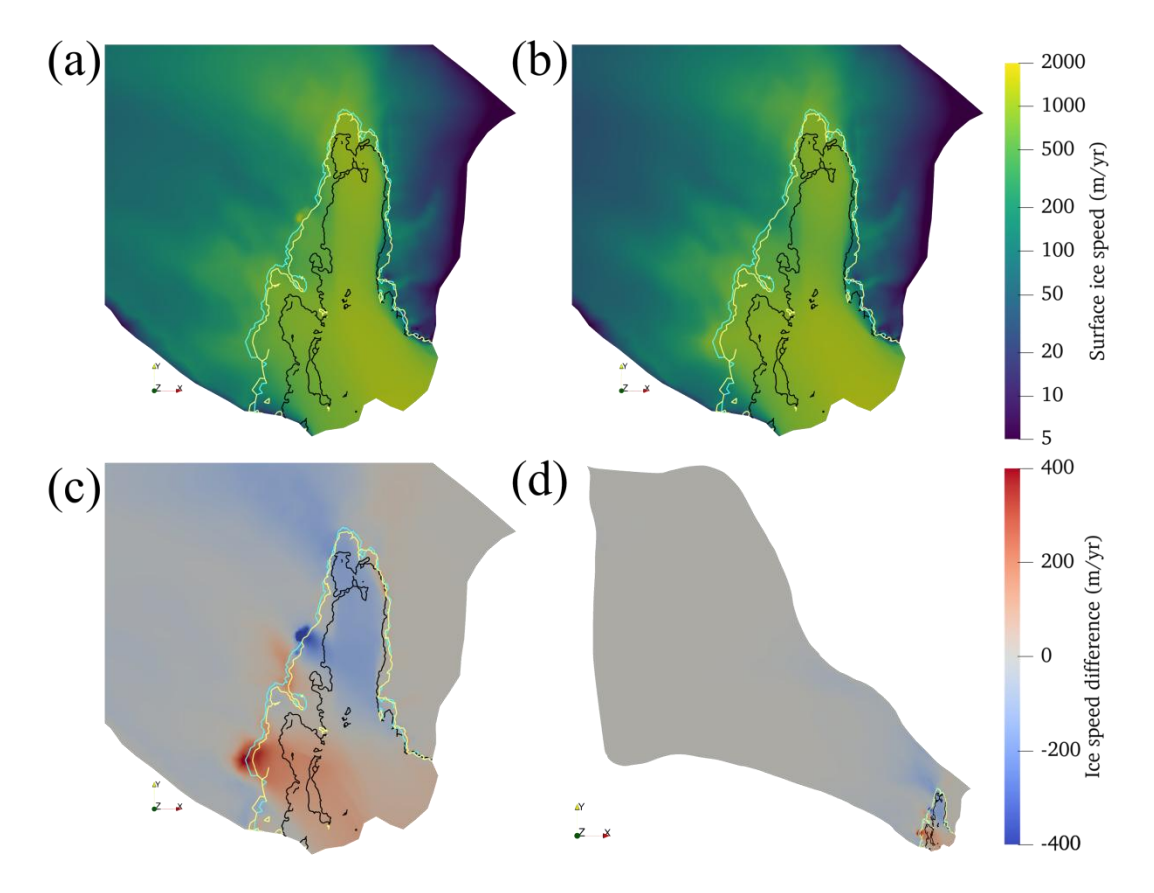


Fig. S9. Surface ice speed using 5% overburden effective pressures (a) and assuming perfect hydrostatic connection (b) in the year 2050 from the experiment C_{m80} . Difference (b – a) between (a) and (b) is shown in (c) and (d). The yellow and cyan curves represent the grounding line positions under 5% overburden and perfect hydrostatic connection respectively.